Published in final edited form as:
J Orthop Res. 2022 August ; 40(8): 1721–1734. doi:10.1002/jor.25223.

Functional tissue engineering of articular cartilage for biological joint resurfacing – The 2021 Elizabeth Winston Lanier Kappa Delta Award

Farshid Guilak[1,2,3,4], **Bradley T. Estes**[4], **Franklin T. Moutos**[4]

[1]Department of Orthopaedic Surgery, Washington University, St. Louis, MO, USA

[2]Shriners Hospitals for Children – St. Louis, St. Louis, MO, USA

[3]Center of Regenerative Medicine, Washington University, St. Louis, MO, USA

[4]Cytex Therapeutics, Inc., Durham, NC, USA

Abstract

Biological resurfacing of entire articular surfaces represents a challenging strategy for treatment of cartilage degeneration that occurs in osteoarthritis. Not only does this approach require anatomically sized and functional engineered cartilage, but the inflammatory environment within an arthritic joint may also inhibit chondrogenesis and induce degradation of native and engineered cartilage. Here we present the culmination of multiple avenues of interdisciplinary research leading to the development and testing of a bioartificial cartilage for tissue-engineered resurfacing of the hip joint. The work is based on a novel three-dimensional weaving (3D) technology that is infiltrated with specific bioinductive materials and/or genetically-engineered stem cells. A variety of design approaches have been tested *in vitro*, showing biomimetic cartilage-like properties as well as the capability for long-term tunable and inducible drug-delivery. Importantly, these cartilage constructs have the potential to provide mechanical functionality immediately upon implantation, as they will need to replace a majority, if not the entire joint surface in order to restore function. To date, these approaches have shown excellent preclinical success in a variety of animal studies, including the resurfacing of a large osteochondral defect in the canine hip, and are now well-poised for clinical translation.

Keywords

cartilage repair; collagen; proteoglycan; hip; knee; focal defect

Correspondence address: Farshid Guilak, PhD, Department of Orthopaedic Surgery, Washington University in St. Louis, Couch Biomedical Research Building, Room 3213, 4515 McKinley Avenue, St Louis, MO, 63110 USA, guilak@wustl.edu.
Author Contributions: All authors contributed to the writing of this paper. All authors have read and approved the final submitted manuscript.

Conflict of Interest Statement
The authors are employees and shareholders in Cytex Therapeutics, Inc.

Introduction

Under normal physiologic circumstances, articular cartilage functions for decades as a nearly frictionless surface in diarthrodial joints while exposed to loads of several times body weight[1]. This remarkable mechanical function is attributed to the unique structure and composition of the cartilage extracellular matrix (ECM) [2]. In a healthy joint, the compressive, tensile, and viscoelastic properties of hyaline cartilage contribute to load bearing, energy dissipation, and joint lubrication over the lifetime of the joint [3]. However, degeneration of the cartilage is associated with significant loss of cartilage function that contributes to further degeneration of the joint, which ultimately leads to osteoarthritis (OA), a debilitating disease affecting over 27 million people in the United States alone [4]. For patients suffering from end-stage OA of the hip, the standard surgical treatment is total hip arthroplasty (THA), which has proven effective in the aging population. However, only a low percentage of young, active patients opt for THA due to the shortened projected lifespan of a hip implant for an active patient and the subsequent need for revision surgery, which is associated with significant complications, co-morbidities, overall decreased effectiveness, and less patient satisfaction [5–7]. The ability to repair or regenerate cartilage using tissue engineering strategies could have a tremendous impact on the treatment of OA for the growing population of active patients with hip OA. To this end, there has been a significant increase in research and development aimed at improving cartilage repair strategies, which include marrow stimulation, osteochondral transfer, and various forms of autologous chondrocyte implantation. However, these alternative biologic techniques are ineffective for larger lesions [8–12]. Second generation autologous chondrocyte implantation (ACI) or matrix-assisted chondrocyte implantation (MACI) procedures are not approved for use outside the knee joint and report an almost 30% failure rate within 9 years in young patients [9,11,13]. Clearly, there is a need for improved techniques, implants, and procedures to effectively treat the disease or, at a minimum, delay the progression of OA to the point at which the patients are better candidates for a hip arthroplasty procedure.

An important challenge in the development of biological resurfacing techniques for treating OA is the ability to manufacture large engineered tissue constructs with patient-specific geometries that precisely match the native joint surface, while withstanding the harsh mechanical and biochemical environment of the damaged joint. There have been several initial studies aimed at biologic cartilage joint resurfacing [14–17]. Hung and colleagues demonstrated proof of concept for joint resurfacing using young bovine chondrocytes encapsulated in agarose cultured on bovine trabecular bone, and this group later modeled nutrient and diffusion related parameters for growing large-scale constructs [16,17]. In other studies, 3D printed scaffolds were used to recreate joint anatomy in an *in vivo* rabbit model [14,15], showing encouraging data demonstrating that polymer-based porous scaffolds could promote cell attachment and tissue regeneration [14,15,18]. Scaffold-free constructs have also been used in a rabbit model for articular cartilage repair, in which autologous chondrocytes are expanded *in vitro* to form a neo-cartilage layer [19]. Condensed mesenchymal cell bodies can also be fused together to grow centimeter-sized pieces of human articular cartilage in culture [20]. However, the challenge of providing an implant with biomimetic cartilage properties at the time of initial cell seeding still remains and is needed to address the important clinical need for repair or regeneration of cartilage in patients who have activity-limiting cartilage loss or osteoarthritis but are too young for a total joint replacement.

Here we summarize the culmination of over 15 years of research leading to the development of a bioartificial cartilage for repair or resurfacing of large osteochondral defects, even approaching a biologically-based total joint resurfacing procedure (Figure 1). The primary technology that has served as the basis for this approach has been the development of a novel method for three-dimensional (3D) weaving of microscale biomaterial fibers, allowing the formation of tough yet flexible scaffolds for tissue engineering that allow cellular infiltration but have highly defined anisotropic, nonlinear, and viscoelastic material properties that mimic those of native cartilage. Importantly, the 3D nature of this method allows the formation of large, anatomically-shaped scaffolds that can be used for regeneration of osteochondral tissues in the shape of an entire joint surface. Here, we describe the development and refinement of this 3D weaving method for cartilage and bone tissue engineering, showing excellent functional success in a large animal preclinical study of hip OA.

Three-dimensional weaving of biomaterial scaffolds

The engineered repair of cartilaginous tissues has remained particularly challenging. From a biomechanical standpoint, cartilage can be represented as a multiphasic fiber-reinforced material, with anisotropic, inhomogeneous, nonlinear, and viscoelastic properties [21–23]. The fundamental basis for our technology for biological joint resurfacing has been through the development of a method for 3D weaving of fibers into a biomimetic scaffold that reproduces these functional mechanical properties of articular cartilage [24]. Previous approaches for cartilage tissue engineering have tended to utilize either porous nonwoven scaffolds [25–30], hydrogels [31–37], or a combination of the two[38] that can provide environments supportive of chondrogenesis, but generally cannot provide the complex mechanical properties believed necessary for sustained load support *in vivo* [22]. Furthermore, the mechanical properties of most hydrogel scaffolds, particularly stiffness and strength, are several orders of magnitude lower than those of native cartilage [28,35,39,40], thus requiring prolonged *in vitro* culture to attain native tissue properties before implantation. One approach to developing a scaffold with prescribed mechanical properties while maintaining an environment conducive to cell growth is by using a porous fiber-reinforced composite material that includes separate phases [41–43].

Our primary design goal was to create a novel scaffold for the functional tissue engineering of articular cartilage that qualitatively and quantitatively mimics the behavior and mechanical properties of articular cartilage *a priori*, without the need for extended *in vitro* culture. To this end, a microscale 3D textile manufacturing technique was developed to weave bioresorbable yarns into an orthotropic, porous fabric that could be infiltrated with cells and/or a consolidating hydrogel to yield a composite scaffold (Figure 2). In contrast to standard 2D weaving, which requires lamination of separate layers to achieve the appropriate thickness, 3D weaving involves simultaneous weaving of multiple fiber layers in three orthogonal directions to form a one-piece scaffold structure with regular, interconnected pores. Additional advantages include control of multi-directional (anisotropic) mechanical properties, control of fiber spacing and volume fraction in each axis, and the ability to select each individual fiber in the construct [44]. These design variables provide for a wide range of physical and mechanical properties that can be precisely tuned to match specific tissue characteristics. By altering several of the initial design variables (e.g., material, yarn size, and yarn spacing), a composite scaffold was designed and fabricated with initial mechanical properties that were anisotropic, nonlinear, and viscoelastic, with values of mechanical test parameters that bracketed native articular cartilage *a priori*, even in the absence of cells and ECM.

Initially, 3D textile structures were produced using multi-filament poly(glycolic acid) (PGA) yarn, containing rectangular pores with dimensions of approximately ~400 μm x ~300 μm x ~100 μm and a large void volume of approximately 70–75%. Composite materials were then formed by infusing agarose or fibrin hydrogels into the woven structures using a modified vacuum-assisted molding process. These composite scaffolds exhibited unique mechanical behaviors that were anisotropic, nonlinear, and viscoelastic, thereby mimicking the mechanical behavior of native cartilage. These findings show that a scaffold made from different biocompatible materials previously shown to be conducive to chondrogenesis (e.g., PGA [45], agarose [32], or PGA and fibrin [38]) can be constructed with highly controlled biomechanical properties by virtue of the 3D fiber-reinforcement of the composite structure.

Tissue-engineering of cartilage using 3D woven scaffolds

To examine the ability of these 3D woven scaffolds to support cellular infiltration, cartilage matrix accumulation, and maintenance of biomimetic mechanical properties, we produced 3D woven poly (ε-caprolactone) (PCL, molecular weight 50 – 60 kDa) structures, seeded them with human adipose-derived stem cells (ASCs), suspended in a fibrin hydrogel, and cultured them for 28 days in chondrogenic culture conditions [46,47] (Figure 3). PCL was used due to its excellent biocompatibility and slow degradation rates *in vivo* as compared to PGA, which degrades in 3–4 weeks. Compressive and shear biomechanical testing showed that PCL-based constructs had biomimetic mechanical properties similar to those of native human cartilage at time zero, and they maintained their mechanical properties relative to baseline throughout the culture period, while supporting the synthesis of a collagen-rich extracellular matrix. These findings are in contrast to previous studies that show culture times of 9 weeks or more are needed to achieve near-native cartilage mechanical properties [48]. Furthermore, constructs displayed an equilibrium coefficient of friction similar to that of native articular cartilage (μ_{eq} ~ 0.1 – 0.3) over the prescribed culture period. These findings show proof of concept for the ability of a bioresorbable and biocompatible 3D woven matrix to serve as a functional scaffold for cartilage tissue engineering. We further examined the ability of different cell sources and scaffold structures on the formation of cartilaginous tissues, as well as the ability of bioreactor-based stimulation to enhance these chondrogenic properties [49].

Osteochondral tissue formation on 3D woven scaffolds

There has been extensive interest in tissue-engineering cartilage, bone, or combined osteochondral constructs that can provide enhanced fixation of engineered tissues into the defect site. Thus, an important aspect of our work has been to demonstrate the ability of 3D woven scaffolds to support osteogenesis and bone formation, both *in vitro* and *in vivo* [50–52]. We hypothesized that *in vitro* culture duration and medium additives can individually and interactively influence the structure, composition, mechanical, and molecular properties of tissues that have been engineered with human MSCs cultured on 3D woven PCL [50]. Bone marrow MSCs were suspended in a type I collagen gel, seeded on scaffolds, and cultured for 1, 21, or 45 days in chondrogenic and/or osteogenic conditions. Structure, composition, biomechanical properties, and gene expression were analyzed. In chondrogenic medium, cartilaginous tissue formed by day 21, and hypertrophic mineralization was observed in the newly formed extracellular matrix at the interface with the underlying scaffold by day 45. Hydroxyproline, S-GAGs, calcium content, and alkaline phosphatase activity depended on culture duration and medium additives, with significant interactive effects (all $p<0.0001$). The 45-day constructs exhibited mechanical properties on the order of magnitude of native articular cartilage. Gene expression was characteristic of chondrogenesis and endochondral bone formation, with sequential regulation of *SOX9*, *COL2A1*, *ACAN*, *RUNX2*, *BMP2*, and *BSP*. These findings demonstrated the ability of 3D woven scaffolds to support either MSC chondrogenesis or osteogenesis dependent upon specific culture conditions.

Several previous approaches have demonstrated the ability to develop osteochondral constructs by combining multiple cells types [53–57], multilayered scaffolds [58–62], or multistep differentiation protocols [54,63–69]. However, it is still a major challenge to differentially direct cell fate determination into distinct lineages (i.e., cartilage and bone) from a single cell source, in a single culture system, while utilizing only one scaffold material. If proven efficacious, a single stage approach would streamline the engineering of multiphase tissues by circumventing the need for multiple cell types or multiple differentiation culture conditions. In this regard, members of the transforming growth factor β (TGF-β) family have been extensively utilized in the engineering of skeletal tissues, but it is important to note that these factors have distinct effects on chondrogenic and osteogenic differentiation of progenitor cells. We developed a method to direct human MSCs toward either an osteogenic lineage that exhibits matrix mineralization or a chondrogenesis within the same biochemical environment by culturing cells on engineered 3D woven PCL scaffolds in a chondrogenic environment while inhibiting TGF-β3 signaling through *SMAD3* knockdown, in combination with overexpressing *RUNX2*, a master transcription factor in osteoblast differentiation [51]. The highest levels of mineral deposition and alkaline phosphatase activity were observed on scaffolds with genetically engineered MSCs and exhibited an additive effect in response to *SMAD3* knockdown and *RUNX2* expression. Meanwhile, unmodified MSCs on PCL scaffolds exhibited accumulation of an extracellular matrix rich in S-GAGs and collagen II in the same chondrogenic environment, as expected. This ability to induce differential matrix deposition in a single culture condition opens new avenues for developing complex tissue replacements for cartilage and bone defects.

Finally, to determine if such chondral or osteochondral constructs developed *in vitro* can maintain their phenotype and stability *in vivo*, we determined the ability of MSCs to form cartilage or bone tissue, both in a nude rat subcutaneous pouch model and under simulated conditions *in vitro* [52]. In the first portion of this study, various scaffold permutations, including PCL alone, PCL-bone, “point-of-care” seeded MSC-PCL-bone, and chondrogenically pre-cultured Ch-MSC-PCL-bone constructs were implanted in a dorsal, ectopic pouch in a nude rat (Figure 4). After eight weeks, only cells in the Ch-MSC-PCL constructs exhibited both chondrogenic and osteogenic gene expression profiles. Notably, while both tissue profiles were present, constructs that had been chondrogenically pre-cultured prior to implantation showed a loss of GAGs as well as the presence of mineralization along with the formation of trabecula-like structures. Notably, while both tissue profiles were present, constructs that had been chondrogenically pre-cultured prior to implantation showed a loss of GAGs as well as the presence of mineralization along with the formation of trabecula-like structures, indicating a transition to an osteogenic phenotype of MSCs following in vivo implantation.

Hybrid composite materials made from 3D woven scaffolds

One of the major advantages of this 3D woven structure is that its high porosity and permeability, which results from a regular, interconnected pore network, allow the uniform infiltration of different materials into the structure, along with living cells. This type of approach provides many advantages such as the delivery of bioactive scaffold materials to enhance tissue growth, or the use of consolidating materials such as hydrogels or polymers to further enhance the mechanical properties of the construct[70–73]. Using this approach, we have performed several studies that show that various composite scaffold such as this can not only provide fiber-reinforcement to greatly enhance the properties of chondrogenic hydrogels and materials, but the combination of complex, engineered materials can further enhance the toughness and frictional properties of the 3D woven scaffold.

In previous studies, we have shown that porous scaffolds produced from devitalized, full-thickness porcine cartilage-derived matrix (CDM) can promote the chondrogenic differentiation of seeded ASCs, without the need for exogenously added growth factors [74,75]. However, constructs showed relatively low compressive moduli (~50 kPa at day 0), and cell-seeded scaffolds contracted significantly over time. Based on these findings, we hypothesized that CDM could be combined with a 3D woven PCL reinforcement to form a functional, bioactive scaffold system capable of inducing a cartilaginous phenotype in ASCs [72] (Figure 5). 3D woven PCL scaffolds were infiltrated with a slurry of homogenized porcine CDM, seeded with human ASCs, and cultured for up to 42 days in standard growth conditions. While all scaffolds promoted a chondrogenic phenotype of the ASCs, CDM-only scaffolds showed low compressive and shear moduli and contracted significantly during culture. Fiber-reinforced CDM scaffolds and 3D woven PCL scaffolds maintained their mechanical properties and initial size and shape throughout the culture period, while supporting the accumulation of a cartilaginous extracellular matrix. These findings show that fiber-reinforced hybrid scaffolds can be produced with biomimetic mechanical properties, as well as the ability to promote ASC differentiation and chondrogenesis *in vitro.* Similarly, we have shown that infiltrating the 3D woven PCL scaffold with a self-assembling peptide (RAD16-I, also known as “Puramatrix”) can promote the re-differentiation of dedifferentiated chondrocytes and maintain the initial shape and viscoelastic behavior throughout the culture period, while constructs with RAD16-I scaffold alone contract during culture time into a stiffer and compacted structure.[73].

In addition to regulating cell behavior, an infiltrating hydrogel or polymer in the 3D woven scaffold can be used to "consolidate" the fibers and significantly alter or enhance their mechanical behavior. To test this process, 3D woven scaffolds were infiltrated with various interpenetrating network (IPN) hydrogels, which consist of two different polymers that are mixed with one another at the molecular scale (Figure 5). These polymers are especially attractive as they exhibit synergistically increased fracture toughness and tribological properties as compared to the individual components of the network [76]. We found that infusion of the 3D woven PCL scaffold with IPNs of alginate/polyacrylamide (Alg/PAAm) or fibrin/PAAm significantly increased the Young's modulus over the PCL scaffold alone [70]. Specifically, the aggregate modulus of the Alg/PAAm IPN (~0.4 MPa) was significantly higher than that of the single network hydrogel of alginate or PAAm separately. However, the reinforcement of the hydrogel with the 3D woven scaffold resulted in a further improvement in the modulus of the composite construct, with values reaching approximately 1.2 MPa for 3D woven PCL infiltrated with Alg/PAAm IPN and 0.9 MPa for the 3D woven PCL infiltrated with fibrin/PAAm IPNs, which were significantly higher than the PCL scaffold alone (Figure 5). This finding suggests that the interaction of the IPN hydrogels with the 3D woven PCL scaffold was responsible for the improvement in mechanical strength, a departure from conventional interpretation of fiber reinforced gel networks, in which the fiber components generally serve as the strength determinant [70].

In follow-up studies to this work, we developed an agarose and poly(ethylene) glycol IPN hydrogel that showed high viability of MSCs within the IPN hydrogel, with improved mechanical properties compared to constructs comprised of individual components [71]. We further strengthened these properties by integrating the hydrogel with a 3D woven structure. The resulting fiber-reinforced hydrogels displayed functional macroscopic mechanical properties mimicking those of native articular cartilage, while providing a local microenvironment that supports cellular viability and function. These findings suggest that a fiber-reinforced IPN hydrogel can support stem cell chondrogenesis while allowing for significantly enhanced, complex mechanical properties at multiple scales as compared to individual hydrogel or fiber components.

Scaffold-mediated viral delivery for spatial and temporal control of cell behavior

While many tissue-engineering approaches are based on the delivery of stem or progenitor cells on scaffolds, the differentiation of these cells can require extensive *in vitro* manipulation and costly growth factor delivery. Furthermore, upon implantation *in vivo*, the ability to further specify or modify cell fate is lost. Thus, the ability to induce and maintain stem cell differentiation *in vivo* over extended periods of time in the absence of exogenous growth factors could significantly enhance tissue regeneration. To address this issue, we developed a method to functionally immobilize lentiviral particles precisely to individual fibers of the 3D woven scaffold using poly-L-lysine (PLL) (Figure 6) [51,77,78]. This approach allows site-specific transduction of cells that are seeded on the scaffold, while preventing the virus from affecting other cells.

Scaffold-mediated transduction of MSCs with lentiviral vectors driving expression of TGF-β3 led to potent chondrogenic differentiation and accumulation of a cartilaginous ECM rich in type II collagen and S-GAGs, both of which are major components of articular cartilage [77]. By nearly all measures of gene regulation, protein content, and biomechanical properties, the level of chondrogenic differentiation achieved at day 28 by immobilizing lentivirus was indistinguishable from that using exogenous TGF-β3 treatment [77].

In addition to delivering genes for the production and directed regulation of anabolic growth factors [51,77], we have also used this approach to create tunable and inducible systems for delivery of cytokine inhibitors [78]. For example, there is ample evidence indicating that proinflammatory cytokines, and particularly interleukin 1 (IL-1), play an important role in the pathogenesis of OA [79–81] as well as the inhibition of mesenchymal stem cell (MSC)-based repair of cartilage [82–87]. While we have demonstrated that the overall mechanical functionality of cartilage engineered tissue in the presence of pathophysiological levels of IL-1[88] can be preserved through the use of a 3D woven scaffold, exposure to this cytokine significantly inhibits the chondrogenic development and maturation of MSC-synthesized ECM [89]. As a means of inhibiting the effects of such an inflammatory environment on engineered cartilage, we used this lentivirus-immobilization technique to create a tunable and inducible gene delivery system for IL-1 receptor antagonist (IL-1Ra)[78], the inhibitor of IL-1 (Figure 6). A doxycycline-inducible vector was used to transduce MSCs within the 3D woven PCL scaffolds to enable tunable IL-1Ra production. In the presence of IL-1, IL-1Ra-expressing engineered cartilage produced cartilage-specific extracellular matrix, while resisting IL-1-induced upregulation of matrix metalloproteinases and maintaining mechanical properties similar to native articular cartilage [78]. The ability of functional engineered cartilage to self-tune the delivery of anti-inflammatory cytokines to the joint may enhance the long-term success of therapies for cartilage injuries or osteoarthritis.

Anatomically shaped tissue-engineered cartilage for biological joint resurfacing

Biological resurfacing of entire articular surfaces represents a novel but challenging strategy for treatment of cartilage degeneration that occurs in osteoarthritis. Not only does this approach require anatomically sized and functional engineered cartilage, but the inflammatory environment within an arthritic joint may also inhibit chondrogenesis and induce degradation of native and engineered cartilage. To address these issues, we used adult stem cells to engineer anatomically shaped, functional cartilage constructs capable of tunable and inducible expression of anti-inflammatory molecules, specifically IL-1Ra [90]. Large (22 mm diameter) hemispherical scaffolds were fabricated from 3D woven PCL fibers into two different configurations and were seeded with human ASCs (Figure 7). Doxycycline(dox)-inducible lentiviral vectors containing eGFP or IL-1Ra transgenes were immobilized to the PCL to transduce ASCs upon seeding, and constructs were cultured in chondrogenic conditions for 28 days.

Constructs showed biomimetic cartilage properties and uniform tissue growth while maintaining their anatomic shape throughout culture. IL-1Ra-expressing constructs produced nearly 1 μg/mL of IL-1Ra upon controlled induction with dox. Treatment with IL-1 significantly increased MMP activity in the conditioned media of eGFP-expressing constructs but not in IL-1Ra-expressing constructs [90]. Our findings show that advanced textile manufacturing combined with scaffold-mediated gene delivery can be used to tissue-engineer large anatomically shaped cartilage constructs, in the shape of a hip or knee condyle, that possess controlled delivery of anti-cytokine therapy. Moreover, these cartilage constructs have the potential to provide mechanical functionality immediately upon implantation, a critically important characteristic, as they will need to replace a majority, if not the entire joint surface, in order to restore function.

Biological resurfacing in a large animal, preclinical model of hip osteoarthritis

Given the success and proof-of-concept in all aspects of this work *in vitro* and in small animal orthotopic sites, we next sought to test the ability of 3D woven, tissue-engineered osteochondral construct to resurface a massive defect on the femoral head of the hip and to restore the biomechanical function of the tissue and the whole joint [91]. An important step in this process was the development of a bicomponent scaffold consisting of the 3D woven textile described in the previous section, bonded to a 3D printed osteoconductive PCL base for direct fixation into the femoral head. Autologous bone marrow derived mesenchymal stem cells (MSCs) were harvested, expanded in culture, seeded on the scaffold, and differentiated using a chondrogenic cocktail containing TGF-β3 for 4 weeks (Figure 8). To minimize potential regulatory issues, gene therapy approaches were not used in this preclinical study. A 10 mm in diameter x 2 mm deep osteochondral lesion was created on the dorsal, load bearing aspect of the femoral head (where canine hip OA typically develops) in skeletally-mature purpose-bred hounds and repaired with the cell-seeded implant matching the anatomical joint surface curvature. For control animals, this defect was left empty. The implants showed success in all measured outcomes. The dogs that received the engineered implant returned to normal activity levels by 6 months as measured by their activity during the day, averaged over a 2-week period, whereas the control cohort did not return to normal activity levels by the end of the study. Kinetic gait analysis revealed normal GRFs (peak vertical force [PVF]; vertical impulse [VI]) on the operated limb by 6 months postoperatively in the implant group. Conversely, the control animals displayed clinically observable lameness throughout the study after OA was initiated in the joint and significantly lower GRFs than the implant group. The pain index score, which measures behavior, activity levels, happiness- and anxiety-like behaviors, demonstrated a return to normal behavior by 6 months in the implant group, in direct contrast to the OA control animals.

All implants remained firmly implanted in the osteochondral defect and demonstrated consistent integration with the surrounding cartilage with no evidence of inflammation. In contrast to control defects, the tissue-engineered implants exhibited a smooth surface that matched the gross morphology of the joint, and no macroscopic depressions were noted in the histological sections. Mechanically, the compressive modulus of the repaired cartilage was 10-fold higher than the tissue from control defects and similar to that reported for normal canine hip cartilage. By all outcome metrics – which included activity monitoring, gait/standing analysis, muscle circumference, and behavioral indices – animals receiving the implant returned to normal preoperative values by 6 months postop. Our data, in total, indicate that this engineered implant restored the contour of the femoral head to its native condition and was functioning as intended from a structural, biological, and anatomical viewpoint to restore joint function and relieve pain in a model of hip OA.

Conclusions and Future Directions

The culmination of this research supports the utility of this approach for large-scale cartilage repair in the clinical setting. A primary advantage of this approach is due to the ability to precisely tune the multidirectional mechanical properties during scaffold manufacture, prior to cell seeding, while maintaining a large void fraction to allow cellular infiltration and tissue ingrowth. Further, 3D-orthogonally woven fabrics have the ability to conform to anatomical structures without compromising the mechanical or biological performance of the structure. The orthogonal interconnected pore structure of both the 3D woven scaffold and the bicomponent scaffold utilized in the canine study enable direct and open communication with the surrounding native tissues, enabling solid integration with host tissues. These properties have also proven highly beneficial in the development of novel cell-based implants for that combine synthetic biology with tissue-engineering for autonomous drug delivery capabilities[92]. Future directions are focused on the translation of this technology into clinical trials for the treatment of osteochondral lesions in the hips young patients (i.e., less than 60 years old) for whom there are currently no good therapeutic options, with the goals of further extending this technology to other joints (e.g., knee, ankle, shoulder, etc.). From a technological standpoint, the combination of 3D weaving with 3D printing provides a platform technology that allows for production of anatomically-shaped bicomponent implants with tunable mechanical and biological properties, and we hope to continue to develop new applications of this technology for the treatment of various musculoskeletal conditions.

Acknowledgments

We greatly thank the Kappa Delta Sorority and the AAOS for this award. This work was supported by NIH grants R01 AG46927, R01 AG15768, R01 AR072999, P30 AR073752, P30 AR074992, and multiple NIH SBIR/STTR grants. We are also indebted to numerous collaborators and colleagues who have contributed to various aspects of this work, including Duncan Lascelles, Masataka Enomoto, Dianne Little, Lisa Freed, Jonathan Brunger, Katherine Glass, William Barefoot, Benjamin Larson, Jean Welter, Arnold Caplan, Nguyen Huynh, Charles Gersbach, Magali Cucchiarini, Henning Madry, Martin Stoddart, Robert Mauck, George Dodge, Alison Ross, Lourdes Recha-Sancho, Carlos Semino, Xuanhe Zhao, I-Chien Liao, Pia Valonen, Christoph Abrahamson, Robert Langer, Sara Oswald, Christopher Rowland, as well as many other collaborators and co-authors. We are also grateful to Christine Estes and Vincent Willard for their continued contributions to this work.

References

1. Guilak F, Setton LA, Kraus VB. 2000. Structure and function of articular cartilage. Principles And Practice Of Orthopaedic Sports Medicine Pg.
2. Heinegård D, Oldberg A. 1989. Structure and biology of cartilage and bone matrix noncollagenous macromolecules. FASEB Journal 3:2042–2051. [PubMed: 2663581]
3. Elliott DM, Guilak F, Vail TP, et al. 1999. Tensile properties of articular cartilage are altered by meniscectomy in a canine model of osteoarthritis. J Orthop Res 17:503–508. [PubMed: 10459755]
4. Buckwalter JA, Martin JA, Brown TD. 2006. Perspectives on chondrocyte mechanobiology and osteoarthritis. Biorheology 43:603–609. [PubMed: 16912432]
5. Malchau H, Herberts P, Ahnfelt L. 1993. Prognosis of total hip replacement in Sweden. Follow-up of 92,675 operations performed 1978–1990. Acta Orthop Scand 64:497–506. [PubMed: 8237312]
6. Robertsson O, Dunbar M, Pehrsson T, et al. 2000. Patient satisfaction after knee arthroplasty: a report on 27,372 knees operated on between 1981 and 1995 in Sweden. Acta Orthop Scand 71:262–267. [PubMed: 10919297]

7. Berry DJ, Harmsen WS, Cabanela ME, et al. 2002. Twenty-five-year survivorship of two thousand consecutive primary Charnley total hip replacements: factors affecting survivorship of acetabular and femoral components. J Bone Joint Surg Am 84-A:171–177.

8. McNickle AG, Provencher MT, Cole BJ. 2008. Overview of existing cartilage repair technology. Sports Medicine and Arthroscopy Review 16:196–201. [PubMed: 19011550]

9. Filardo G, Vannini F, Marcacci M, et al. 2013. Matrix-Assisted Autologous Chondrocyte Transplantation for Cartilage Regeneration in Osteoarthritic Knees: Results and Failures at Midterm Follow-up. Am J Sports Med 41:95–100. [PubMed: 23104612]

10. Hangody L, Dobos J, Balo E, et al. 2010. Clinical experiences with autologous osteochondral mosaicplasty in an athletic population: a 17-year prospective multicenter study. Am J Sports Med 38:1125–1133. [PubMed: 20360608]

11. Niemeyer P, Lenz P, Kreuz PC, et al. 2010. Chondrocyte-seeded type I/III collagen membrane for autologous chondrocyte transplantation: prospective 2-year results in patients with cartilage defects of the knee joint. Arthroscopy 26:1074–1082. [PubMed: 20678705]

12. Saris DB, Vanlauwe J, Victor J, et al. 2009. Treatment of symptomatic cartilage defects of the knee: characterized chondrocyte implantation results in better clinical outcome at 36 months in a randomized trial compared to microfracture. Am J Sports Med 37 Suppl 1:10S–19S. [PubMed: 19846694]

13. Minas T, Gomoll AH, Solhpour S, et al. 2010. Autologous chondrocyte implantation for joint preservation in patients with early osteoarthritis. Clin Orthop Relat Res 468:147–157. [PubMed: 19653049]

14. Woodfield TB, Guggenheim M, von Rechenberg B, et al. 2009. Rapid prototyping of anatomically shaped, tissue-engineered implants for restoring congruent articulating surfaces in small joints. Cell Prolif 42:485–497. [PubMed: 19486014]

15. Lee CH, Cook JL, Mendelson A, et al. 2010. Regeneration of the articular surface of the rabbit synovial joint by cell homing: a proof of concept study. Lancet 376:440–448. [PubMed: 20692530]

16. Hung CT, Lima EG, Mauck RL, et al. 2003. Anatomically shaped osteochondral constructs for articular cartilage repair. Journal of Biomechanics 36:1853–1864. [PubMed: 14614939]

17. Nims RJ, Cigan AD, Albro MB, et al. 2015. Matrix Production in Large Engineered Cartilage Constructs Is Enhanced by Nutrient Channels and Excess Media Supply. Tissue Eng Part C Methods 21:747–757. [PubMed: 25526931]

18. Guilak F. 2010. Homing in on a biological joint replacement. Stem Cell Res Ther 1:40. [PubMed: 21156083]

19. Brenner JM, Ventura NM, Tse MY, et al. 2014. Implantation of scaffold-free engineered cartilage constructs in a rabbit model for chondral resurfacing. Artif Organs 38:E21–32. [PubMed: 24571514]

20. Bhumiratana S, Eton RE, Oungoulian SR, et al. 2014. Large, stratified, and mechanically functional human cartilage grown in vitro by mesenchymal condensation. Proc Natl Acad Sci U S A 111:6940–6945. [PubMed: 24778247]

21. Mow VC, Kuei SC, Lai WM, et al. 1980. Biphasic creep and stress relaxation of articular cartilage in compression? Theory and experiments. J Biomech Eng 102:73–84. [PubMed: 7382457]

22. Soltz MA, Ateshian GA. 2000. A conewise linear elasticity mixture model for the analysis of tension-compression nonlinearity in articular cartilage. J Biomech Eng 122:576–586. [PubMed: 11192377]

23. Woo SL, Lubock P, Gomez MA, et al. 1979. Large deformation nonhomogeneous and directional properties of articular cartilage in uniaxial tension. J Biomech 12:437–446. [PubMed: 457697]

24. Moutos FT, Freed LE, Guilak F. 2007. A biomimetic three-dimensional woven composite scaffold for functional tissue engineering of cartilage. Nat Mater 6:162–167. [PubMed: 17237789]

25. Freed LE, Marquis JC, Nohria A, et al. 1993. Neocartilage formation in vitro and in vivo using cells cultured on synthetic biodegradable polymers. Journal of Biomedical Materials Research 27:11–23. [PubMed: 8380593]

26. Freed LE, Langer R, Martin I, et al. 1997. Tissue engineering of cartilage in space. Proc Natl Acad Sci U S A 94:13885–13890. [PubMed: 9391122]

27. Gao J, Dennis JE, Solchaga LA, et al. 2002. Repair of osteochondral defect with tissue-engineered two-phase composite material of injectable calcium phosphate and hyaluronan sponge. Tissue Eng 8:827–837. [PubMed: 12459061]
28. Pei M, Solchaga LA, Seidel J, et al. 2002. Bioreactors mediate the effectiveness of tissue engineering scaffolds. Faseb J 16:1691–1694. [PubMed: 12207008]
29. Vunjak-Novakovic G, Martin I, Obradovic B, et al. 1999. Bioreactor cultivation conditions modulate the composition and mechanical properties of tissue-engineered cartilage. J Orthop Res 17:130–138. [PubMed: 10073657]
30. Tognana E, Padera RF, Chen F, et al. 2005. Development and remodeling of engineered cartilage-explant composites in vitro and in vivo. Osteoarthritis Cartilage 13:896–905. [PubMed: 16019238]
31. Atala A, Cima LG, Kim W, et al. 1993. Injectable alginate seeded with chondrocytes as a potential treatment for vesicoureteral reflux. J Urol 150:745–747. [PubMed: 8326638]
32. Buschmann MD, Gluzband YA, Grodzinsky AJ, et al. 1992. Chondrocytes in agarose culture synthesize a mechanically functional extracellular matrix. J Orthop Res 10:745–758. [PubMed: 1403287]
33. Caterson EJ, Li WJ, Nesti LJ, et al. 2002. Polymer/alginate amalgam for cartilage-tissue engineering. Ann N Y Acad Sci 961:134–138. [PubMed: 12081882]
34. Kisiday J, Jin M, Kurz B, et al. 2002. Self-assembling peptide hydrogel fosters chondrocyte extracellular matrix production and cell division: implications for cartilage tissue repair. Proc Natl Acad Sci U S A 99:9996–10001. [PubMed: 12119393]
35. Mauck RL, Soltz MA, Wang CC, et al. 2000. Functional tissue engineering of articular cartilage through dynamic loading of chondrocyte-seeded agarose gels. J Biomech Eng 122:252–260. [PubMed: 10923293]
36. Paige KT, Cima LG, Yaremchuk MJ, et al. 1996. De novo cartilage generation using calcium alginate-chondrocyte constructs. Plastic & Reconstructive Surgery 97:168–180. [PubMed: 8532775]
37. Rowley JA, Madlambayan G, Mooney DJ. 1999. Alginate hydrogels as synthetic extracellular matrix materials. Biomaterials 20:45–53. [PubMed: 9916770]
38. Ameer GA, Mahmood TA, Langer R. 2002. A biodegradable composite scaffold for cell transplantation. J Orthop Res 20:16–19. [PubMed: 11853084]
39. LeRoux MA, Guilak F, Setton LA. 1999. Compressive and shear properties of alginate gel: effects of sodium ions and alginate concentration. J Biomed Mater Res 47:46–53. [PubMed: 10400879]
40. Smidsrod O, Skjak-Braek G. 1990. Alginate as immobilization matrix for cells. Trends Biotechnol 8:71–78. [PubMed: 1366500]
41. Hollister SJ. 2005. Porous scaffold design for tissue engineering. Nat Mater 4:518–524. [PubMed: 16003400]
42. Aufderheide AC, Athanasiou KA. 2005. Comparison of scaffolds and culture conditions for tissue engineering of the knee meniscus. Tissue Eng 11:1095–1104. [PubMed: 16144445]
43. Marijnissen WJ, van Osch GJ, Aigner J, et al. 2002. Alginate as a chondrocyte-delivery substance in combination with a non-woven scaffold for cartilage tissue engineering. Biomaterials 23:1511–1517. [PubMed: 11833491]
44. Mohamed MH, Bogdanovich AE, Dickinson LC, et al. 2001. A new generation of 3D woven fabric preforms and composites. Sampe Journal 37:8–17.
45. Freed LE, Vunjak-Novakovic G, Biron RJ, et al. 1994. Biodegradable polymer scaffolds for tissue engineering. Biotechnology (N Y) 12:689–693. [PubMed: 7764913]
46. Estes BT, Wu AW, Storms RW, et al. 2006. Extended passaging, but not aldehyde dehydrogenase activity, increases the chondrogenic potential of human adipose-derived adult stem cells. J Cell Physiol 209:987–995. [PubMed: 16972251]
47. Moutos FT, Guilak F. 2010. Functional properties of cell-seeded three-dimensionally woven poly(epsilon-caprolactone) scaffolds for cartilage tissue engineering. Tissue Eng Part A 16:1291–1301. [PubMed: 19903085]
48. Kim M, Erickson IE, Choudhury M, et al. 2012. Transient exposure to TGF-beta3 improves the functional chondrogenesis of MSC-laden hyaluronic acid hydrogels. J Mech Behav Biomed Mater 11:92–101. [PubMed: 22658158]

49. Valonen PK, Moutos FT, Kusanagi A, et al. 2010. In vitro generation of mechanically functional cartilage grafts based on adult human stem cells and 3D-woven poly(epsilon-caprolactone) scaffolds. Biomaterials 31:2193–2200. [PubMed: 20034665]
50. Abrahamsson CK, Yang F, Park H, et al. 2010. Chondrogenesis and mineralization during in vitro culture of human mesenchymal stem cells on three-dimensional woven scaffolds. Tissue Eng Part A 16:3709–3718. [PubMed: 20673022]
51. Huynh NPT, Brunger JM, Gloss CC, et al. 2018. Genetic Engineering of Mesenchymal Stem Cells for Differential Matrix Deposition on 3D Woven Scaffolds. Tissue Eng Part A 24:1531–1544. [PubMed: 29756533]
52. Larson BL, Yu SN, Park H, et al. 2019. Chondrogenic, hypertrophic, and osteochondral differentiation of human mesenchymal stem cells on three-dimensionally woven scaffolds. J Tissue Eng Regen Med 13:1453–1465. [PubMed: 31115161]
53. Lam J, Lu S, Meretoja VV, et al. 2014. Generation of osteochondral tissue constructs with chondrogenically and osteogenically predifferentiated mesenchymal stem cells encapsulated in bilayered hydrogels. Acta Biomater 10:1112–1123. [PubMed: 24300948]
54. Schaefer D, Martin I, Shastri P, et al. 2000. In vitro generation of osteochondral composites. Biomaterials 21:2599–2606. [PubMed: 11071609]
55. Schaefer D, Martin I, Jundt G, et al. 2002. Tissue-engineered composites for the repair of large osteochondral defects. Arthritis Rheum 46:2524–2534. [PubMed: 12355501]
56. Gao J, Dennis JE, Solchaga LA, et al. 2001. Tissue-engineered fabrication of an osteochondral composite graft using rat bone marrow-derived mesenchymal stem cells. Tissue Eng 7:363–371. [PubMed: 11506726]
57. Cao T, Ho KH, Teoh SH. 2003. Scaffold design and in vitro study of osteochondral coculture in a three-dimensional porous polycaprolactone scaffold fabricated by fused deposition modeling. Tissue Eng 9 Suppl 1:S103–112. [PubMed: 14511474]
58. Moutos FT, Guilak F. 2008. Composite scaffolds for cartilage tissue engineering. Biorheology 45:501–512. [PubMed: 18836249]
59. O’Shea TM, Miao X. 2008. Bilayered scaffolds for osteochondral tissue engineering. Tissue Eng Part B Rev 14:447–464. [PubMed: 18844605]
60. Khanarian NT, Haney NM, Burga RA, et al. 2012. A functional agarose-hydroxyapatite scaffold for osteochondral interface regeneration. Biomaterials 33:5247–5258. [PubMed: 22531222]
61. Khanarian NT, Jiang J, Wan LQ, et al. 2012. A hydrogel-mineral composite scaffold for osteochondral interface tissue engineering. Tissue Eng Part A 18:533–545. [PubMed: 21919797]
62. Cunniffe GM, Gonzalez-Fernandez T, Daly A, et al. 2017. Three-Dimensional Bioprinting of Polycaprolactone Reinforced Gene Activated Bioinks for Bone Tissue Engineering. Tissue Eng Part A.
63. Guo X, Park H, Liu G, et al. 2009. In vitro generation of an osteochondral construct using injectable hydrogel composites encapsulating rabbit marrow mesenchymal stem cells. Biomaterials 30:2741–2752. [PubMed: 19232711]
64. Guo X, Liao J, Park H, et al. 2010. Effects of TGF-beta3 and preculture period of osteogenic cells on the chondrogenic differentiation of rabbit marrow mesenchymal stem cells encapsulated in a bilayered hydrogel composite. Acta Biomater 6:2920–2931. [PubMed: 20197126]
65. Cheng HW, Luk KD, Cheung KM, et al. 2011. In vitro generation of an osteochondral interface from mesenchymal stem cell-collagen microspheres. Biomaterials 32:1526–1535. [PubMed: 21093047]
66. Grayson WL, Bhumiratana S, Grace Chao PH, et al. 2010. Spatial regulation of human mesenchymal stem cell differentiation in engineered osteochondral constructs: effects of pre-differentiation, soluble factors and medium perfusion. Osteoarthritis Cartilage 18:714–723. [PubMed: 20175974]
67. Re’em T, Witte F, Willbold E, et al. 2012. Simultaneous regeneration of articular cartilage and subchondral bone induced by spatially presented TGF-beta and BMP-4 in a bilayer affinity binding system. Acta Biomater 8:3283–3293. [PubMed: 22617742]

68. Chen J, Chen H, Li P, et al. 2011. Simultaneous regeneration of articular cartilage and subchondral bone in vivo using MSCs induced by a spatially controlled gene delivery system in bilayered integrated scaffolds. Biomaterials 32:4793–4805. [PubMed: 21489619]
69. Tuli R, Nandi S, Li WJ, et al. 2004. Human mesenchymal progenitor cell-based tissue engineering of a single-unit osteochondral construct. Tissue Eng 10:1169–1179. [PubMed: 15363173]
70. Liao IC, Moutos FT, Estes BT, et al. 2013. Composite three-dimensional woven scaffolds with interpenetrating network hydrogels to create functional synthetic articular cartilage. Adv Funct Mater 23:5833–5839. [PubMed: 24578679]
71. Moffat KL, Goon K, Moutos FT, et al. 2018. Composite Cellularized Structures Created from an Interpenetrating Polymer Network Hydrogel Reinforced by a 3D Woven Scaffold. Macromol Biosci 18:e1800140.
72. Moutos FT, Estes BT, Guilak F. 2010. Multifunctional hybrid three-dimensionally woven scaffolds for cartilage tissue engineering. Macromol Biosci 10:1355–1364. [PubMed: 20857388]
73. Recha-Sancho L, Moutos FT, Abella J, et al. 2016. Dedifferentiated Human Articular Chondrocytes Redifferentiate to a Cartilage-Like Tissue Phenotype in a Poly(epsilon-Caprolactone)/Self-Assembling Peptide Composite Scaffold. Materials (Basel) 9.
74. Cheng NC, Estes BT, Awad HA, et al. 2009. Chondrogenic differentiation of adipose-derived adult stem cells by a porous scaffold derived from native articular cartilage extracellular matrix. Tissue Eng Part A 15:231–241. [PubMed: 18950290]
75. Diekman BO, Rowland CR, Caplan AI, et al. 2009. Chondrogenesis of adult stem cells from adipose tissue and bone marrow: Induction by growth factors and cartilage derived matrix. Tissue Eng Part A.
76. Gong JP, Kurokawa T, Narita T, et al. 2001. Synthesis of hydrogels with extremely low surface friction. J Am Chem Soc 123:5582–5583. [PubMed: 11389644]
77. Brunger JM, Huynh NP, Guenther CM, et al. 2014. Scaffold-mediated lentiviral transduction for functional tissue engineering of cartilage. Proc Natl Acad Sci U S A 111:E798–806. [PubMed: 24550481]
78. Glass KA, Link JM, Brunger JM, et al. 2014. Tissue-engineered cartilage with inducible and tunable immunomodulatory properties. Biomaterials 35:5921–5931. [PubMed: 24767790]
79. Kapoor M, Martel-Pelletier J, Lajeunesse D, et al. 2011. Role of proinflammatory cytokines in the pathophysiology of osteoarthritis. Nat Rev Rheumatol 7:33–42. [PubMed: 21119608]
80. Teunis T, Beekhuizen M, Van Osch GV, et al. 2014. Soluble mediators in posttraumatic wrist and primary knee osteoarthritis. Arch Bone Jt Surg 2:146–150. [PubMed: 25386573]
81. Sugita T, Kikuchi Y, Aizawa T, et al. 2015. Quality of life after bilateral total knee arthroplasty determined by a 3-year longitudinal evaluation using the Japanese knee osteoarthritis measure. J Orthop Sci 20:137–142. [PubMed: 25209442]
82. Wehling N, Palmer GD, Pilapil C, et al. 2009. Interleukin-1beta and tumor necrosis factor alpha inhibit chondrogenesis by human mesenchymal stem cells through NF-kappaB-dependent pathways. Arthritis Rheum 60:801–812. [PubMed: 19248089]
83. Scotti C, Osmokrovic A, Wolf F, et al. 2012. Response of human engineered cartilage based on articular or nasal chondrocytes to interleukin-1beta and low oxygen. Tissue engineering Part A 18:362–372. [PubMed: 21902467]
84. Kruger JP, Endres M, Neumann K, et al. 2012. Chondrogenic differentiation of human subchondral progenitor cells is affected by synovial fluid from donors with osteoarthritis or rheumatoid arthritis. J Orthop Surg Res 7:10. [PubMed: 22414301]
85. Joos H, Wildner A, Hogrefe C, et al. 2013. Interleukin-1 beta and tumor necrosis factor alpha inhibit migration activity of chondrogenic progenitor cells from non-fibrillated osteoarthritic cartilage. Arthritis Res Ther 15:R119. [PubMed: 24034344]
86. Heldens GT, Blaney Davidson EN, Vitters EL, et al. 2012. Catabolic factors and osteoarthritis-conditioned medium inhibit chondrogenesis of human mesenchymal stem cells. Tissue Eng Part A 18:45–54. [PubMed: 21770865]
87. Djouad F, Bony C, Canovas F, et al. 2009. Transcriptomic analysis identifies Foxo3A as a novel transcription factor regulating mesenchymal stem cell chrondrogenic differentiation. Cloning Stem Cells 11:407–416. [PubMed: 19751111]

88. McNulty AL, Rothfusz NE, Leddy HA, et al. 2013. Synovial fluid concentrations and relative potency of interleukin-1 alpha and beta in cartilage and meniscus degradation. J Orthop Res 31:1039–1045. [PubMed: 23483596]

89. Ousema PH, Moutos FT, Estes BT, et al. 2012. The inhibition by interleukin 1 of MSC chondrogenesis and the development of biomechanical properties in biomimetic 3D woven PCL scaffolds. Biomaterials 33:8967–8974. [PubMed: 22999467]

90. Moutos FT, Glass KA, Compton SA, et al. 2016. Anatomically shaped tissue-engineered cartilage with tunable and inducible anticytokine delivery for biological joint resurfacing. Proc Natl Acad Sci U S A 113:E4513–4522. [PubMed: 27432980]

91. Estes BT, Enomoto M, Moutos FT, et al. 2021. Biological resurfacing in a canine model of hip osteoarthritis. Sci Adv 7:eabi5918.

92. Choi YR, Collins KH, Springer LE, et al. 2021. A genome-engineered bioartificial implant for autoregulated anticytokine drug delivery. Sci Adv 7:eabj1414.

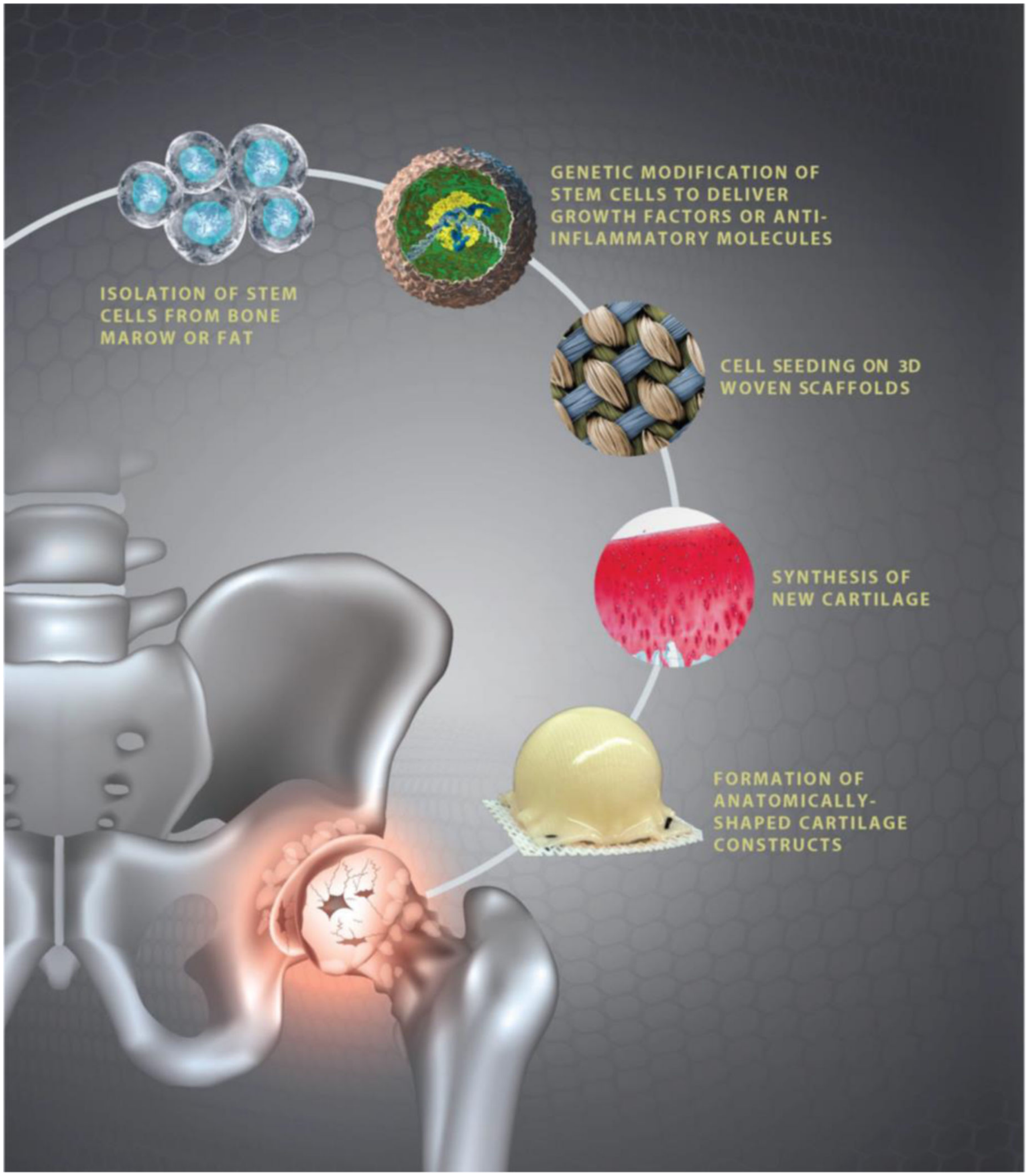

Figure 1. Overview of treatment paradigm for treat advanced osteochondral disease in the young patient.

The overarching goal of this work has been to develop a tissue-engineering approach for biological resurfacing of the hip by using autologous stem cells (which may or may not be genetically altered ex vivo) and then grown on high-performance 3D woven scaffolds to create anatomically-shaped cartilage or osteochondral constructs for joint resurfacing.

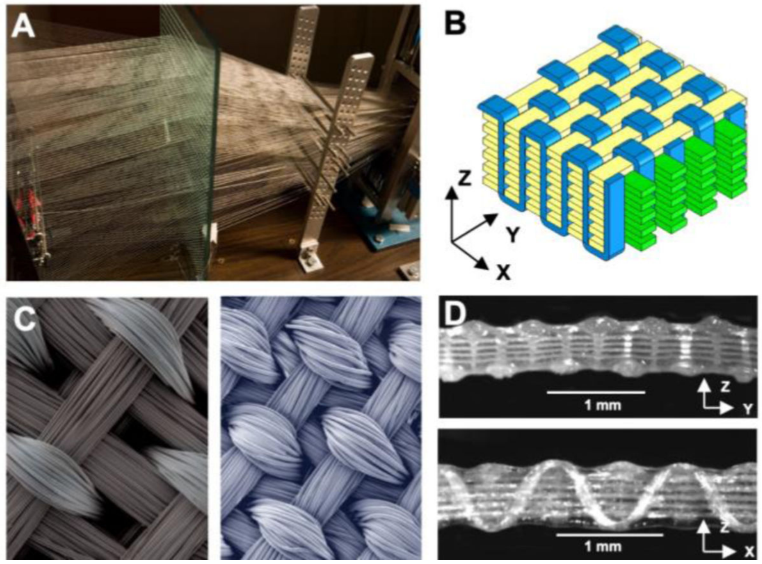

Figure 2. Three-dimensional weaving of biomaterial scaffolds.

The basis of this technology has been the development and construction of a true 3D weaving system. (A) A custom-built 3D loom was designed and built by the authors, allowing simultaneous weaving in x, y, and z directions of 600+ resorbable fibers. (B) The primary architecture used in this work has been a macroporous orthogonal structure. Schematic representation showing x-direction (or warp) fibers in green, y-direction (or weft) fibers in yellow, and z-direction fibers in blue. (C) Surface SEMs of two 3D woven scaffolds produced with different materials and fiber volume fractions (left: PGA fibers; right: PCL fibers). (D) Cross-sections in x (top) and y (bottom) directions showing uniformity of the fabric and pores (PGA fibers). Figure adapted from [24,47].

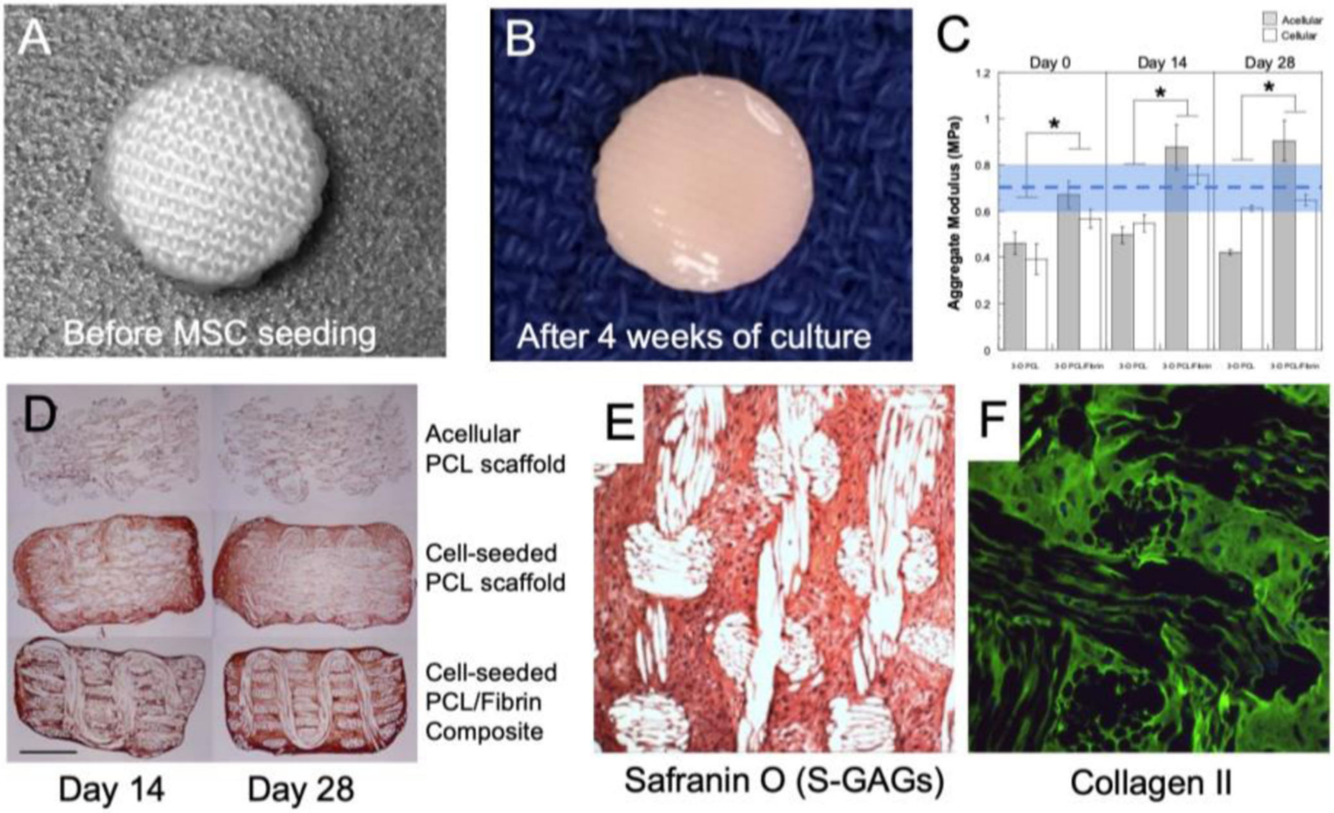

Figure 3. Tissue-engineering of cartilage using 3D woven scaffolds.

(A-B) Macroscopic images of 1cm diameter implant before seeding with human MSCs and after 4 weeks of culture. (C) Compressive aggregate modulus (H_A) of implants seeded with human ASCs and cultured over 4 weeks reveal physiological compressive properties on the order of articular cartilage (dashed line shows typical mean ± s.d. (shaded region) H_A value for human cartilage [21]. The addition of a hydrogel, fibrin, in this case, enhances the development of functional properties. (D) Type II collagen development within the pores structure of the implant is pronounced with and without the addition of fibrin with ASCs cultured on the woven PCL. (E) S-GAG biosynthesis of MSC cultured constructs was enhanced with the use of a bioreactor, and, in dual label-experiments for types I and II collagen, only type II collagen production was observed via fluorescent labeling. Figure adapted from [47,50].

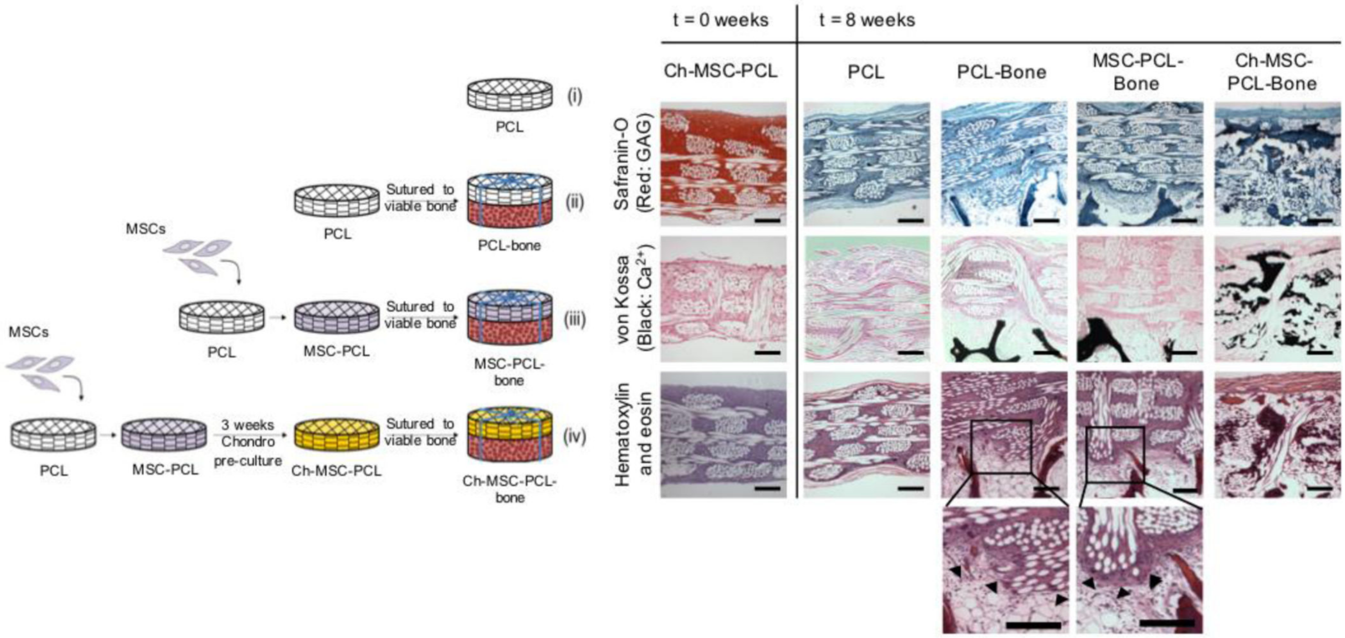

Figure 4. Osteochondral tissue formation on 3D woven scaffolds.

Schematic of experimental setup for ectopic rat study (left) and histological results of the implant disposition at implantation (t=0 weeks) and after 8 weeks (t=8 weeks) in vivo (right). Magnified images (bottom) demonstrate high cellular activity and integration with vital bone (black arrows). Scale bars represent = 200 μm. Figure adapted from [52].

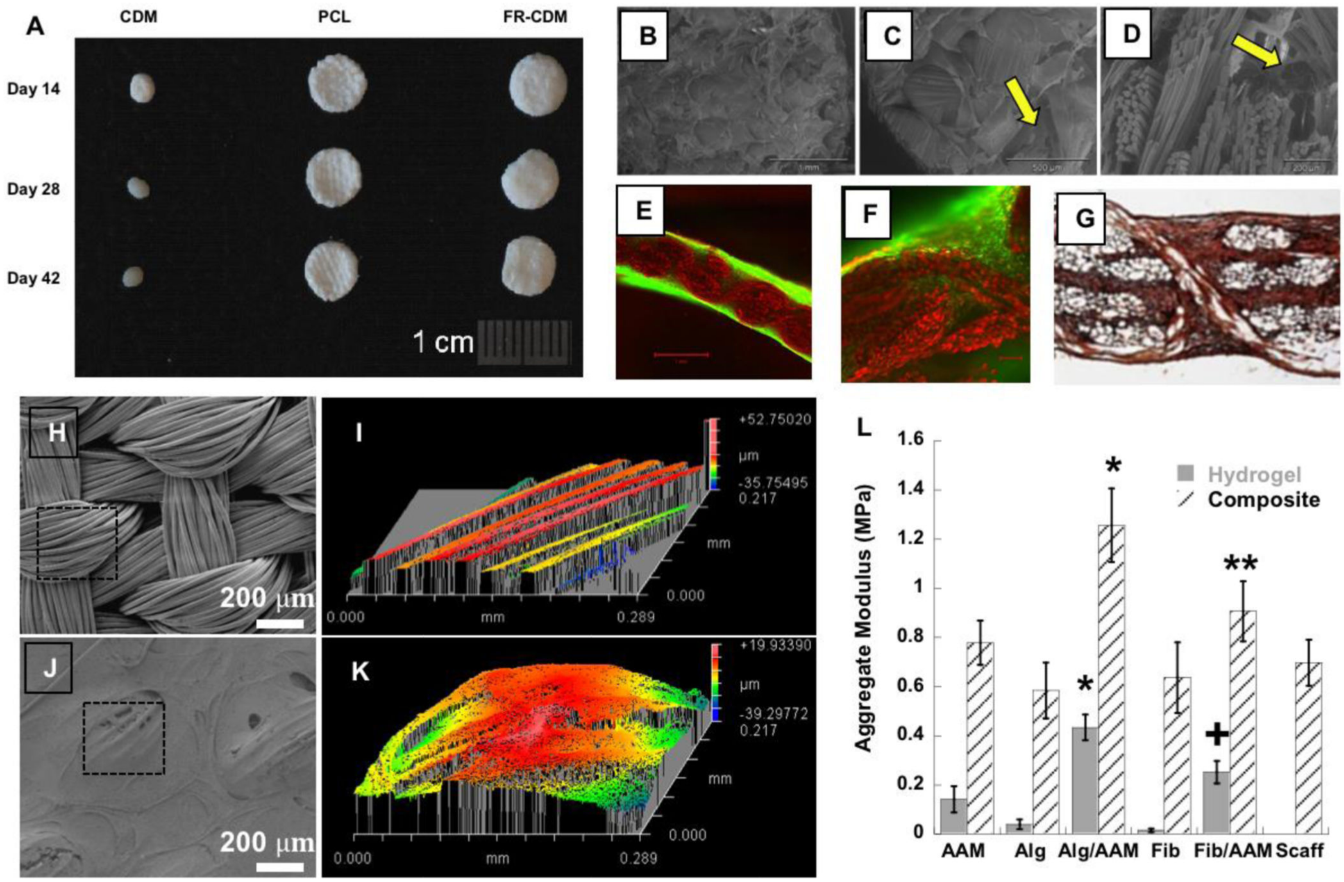

Figure 5. Hybrid composite materials made from 3D woven scaffolds.

(A) Gross morphology of cultured cartilage derived matrix (CDM), PCL, and fiber reinforced CDM (FR-CDM) constructs (6mm diam). PCL and FR-CDM constructs maintained their original size over 42 days of culture, while CDM alone showed marked contraction by day 14. (B,C) Scanning electron microscopy (SEM) surface views and (D) a cross-section of the FR-CDM scaffolds showing CDM within pores of the woven PCL scaffold (arrows). (E-F) Further demonstration of the ability of cells to infiltrate the entire scaffold as indicated by calcein AM labeling (green). (G) Immunolabeling for type II collagen demonstrates abundant type II collagen production throughout the scaffold after 6 weeks of culture. (H-K) SEM and a 3D optical profile of a 3D woven PCL infiltrated with an interpenetrating network (IPN) of alginate and polyacrylamide (Alg/PAAm). These composite surfaces demonstrate the topological smoothing effect of incorporating an IPN within the 3D woven structure. Outlined area in panel H denotes total scanned area in panel I. Outlined area in panel J denotes total scanned area in panel K. (L) Aggregate modulus of IPN and single network hydrogels and their combination with the PCL scaffold to form composites demonstrate increased compressive properties in the composite for the fiber-reinforced IPN (FR-IPN) versus the composites or scaffold alone. ∗$p < 0.05$ for Alg/PAAm composite vs all groups. +$p < 0.05$ for fibrin/polyacrylamide (Fib/PAAm) hydrogel vs all groups. ∗∗$p < 0.05$ for Fib/PAAm composite vs Alginate or Fibrin composites or scaffold alone. Figure adapted from [70,72].

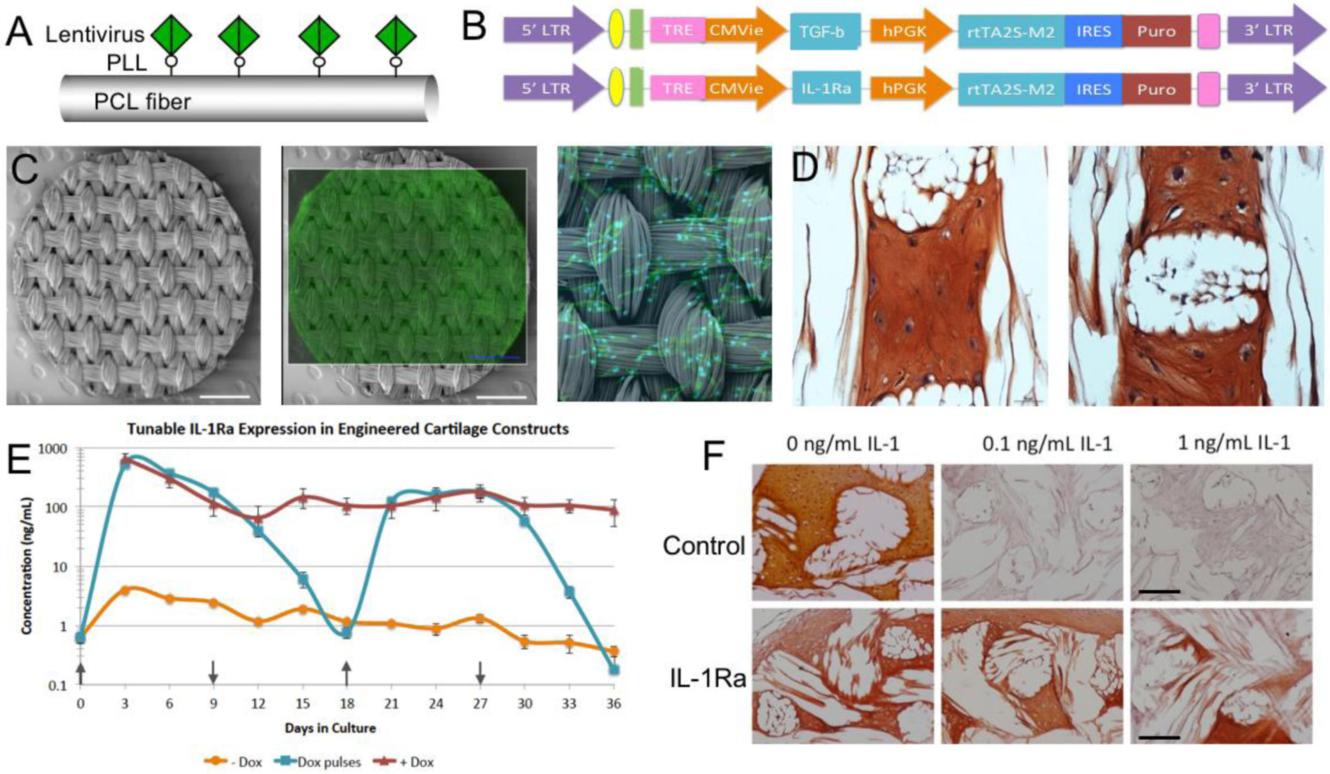

Figure 6. Scaffold-mediated viral delivery for spatial and temporal control of cell behavior

(Top Row) Tunable expression in MSCs with a dox-inducible lentiviral vector. (A) Schematic representation of immobilized lentivirus on PCL fiber. (B) Schematic diagram of lentiviral vectors with TGF-β (top) and IL-1Ra (bottom) as the representative gene of interest. (Middle Row) Scaffold-mediated LV transduction of human MSCs within 3D woven PCL scaffolds (C) SEM image of a 3D woven PCL scaffold 5 mm disk (scale bar = 1mm) and fluorescence image of constitutive eGFP-expressing MSCs on the 3D woven PCL. (D) Scaffold-mediated lentiviral delivery was used to transduce MSCs with the gene for TGF-β, resulting in the production of tissue with a cartilaginous phenotype as demonstrated by Safranin-O red and fast green staining for GAGs and collagen, respectively, without the addition of exogenous TGF-β. (Bottom Row) Tunable IL-1Ra expression in engineered cartilage constructs (E) IL-1Ra secretion from engineered cartilage constructs into media every 72 hours over 36 days of chondrogenesis (mean ± SEM, n=3). +Dox indicates dox induction at 1 μg/mL. -Dox indicates baseline IL-1Ra expression. Arrows indicates when dox (1 μg/mL) was switched on (↑) and off (↓) every 9 days. (F) Safranin-O red and fast green staining showing loss of S-GAGs in Control (non-transduced) cells and protection from IL-1 by IL-1Ra-producing cells. The white space shows the location of the PCL fiber bundles. Figure adapted from [77,78].

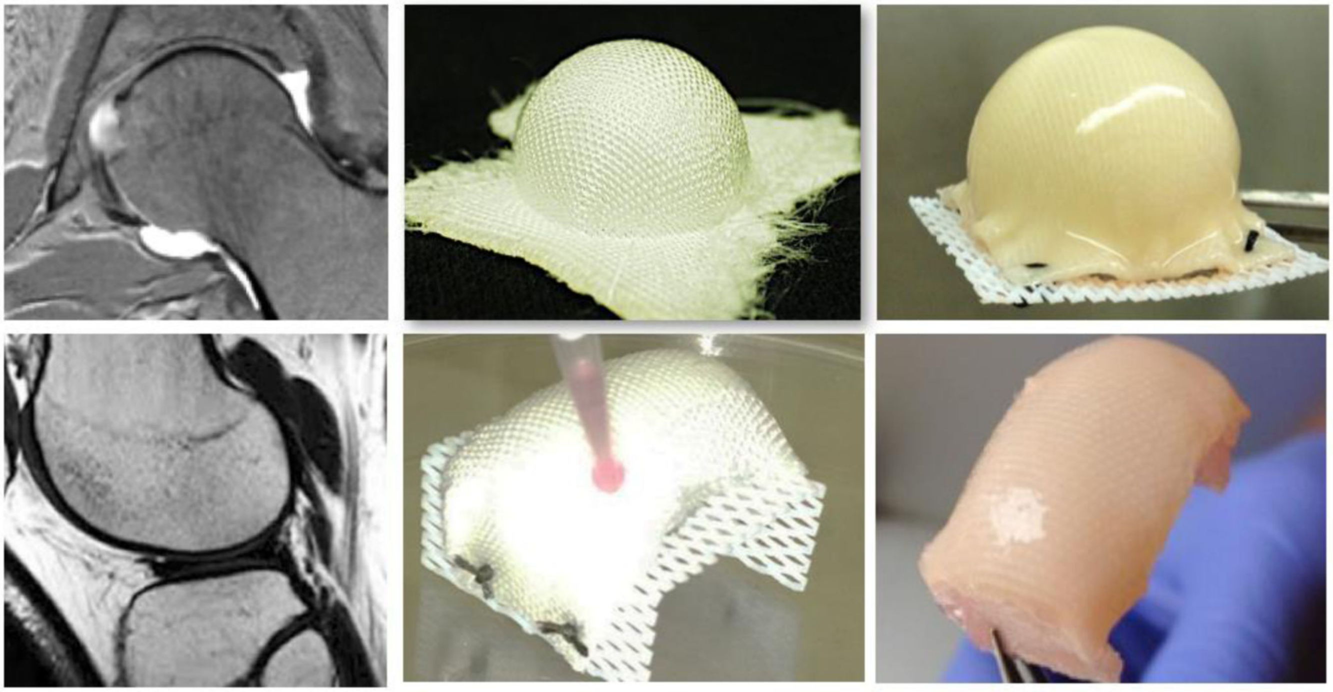

Figure 7. Anatomically shaped tissue-engineered cartilage for biological joint resurfacing of the hip (top) and femoral condyle of the knee (bottom).

(left) Lesions and joint anatomy are mapped from MRI (or CT) and used to prepare an anatomically shaped mold of the hip or knee. (middle) 3D scaffolds were woven from PCL fibers. The implant is formed in a mold, matching anatomical contours of the articular surfaces, and seeded with human ASCs (right). Tissue-engineered hip resurfacing implant culture after 5 weeks of in vitro culture. Figure adapted from [90].

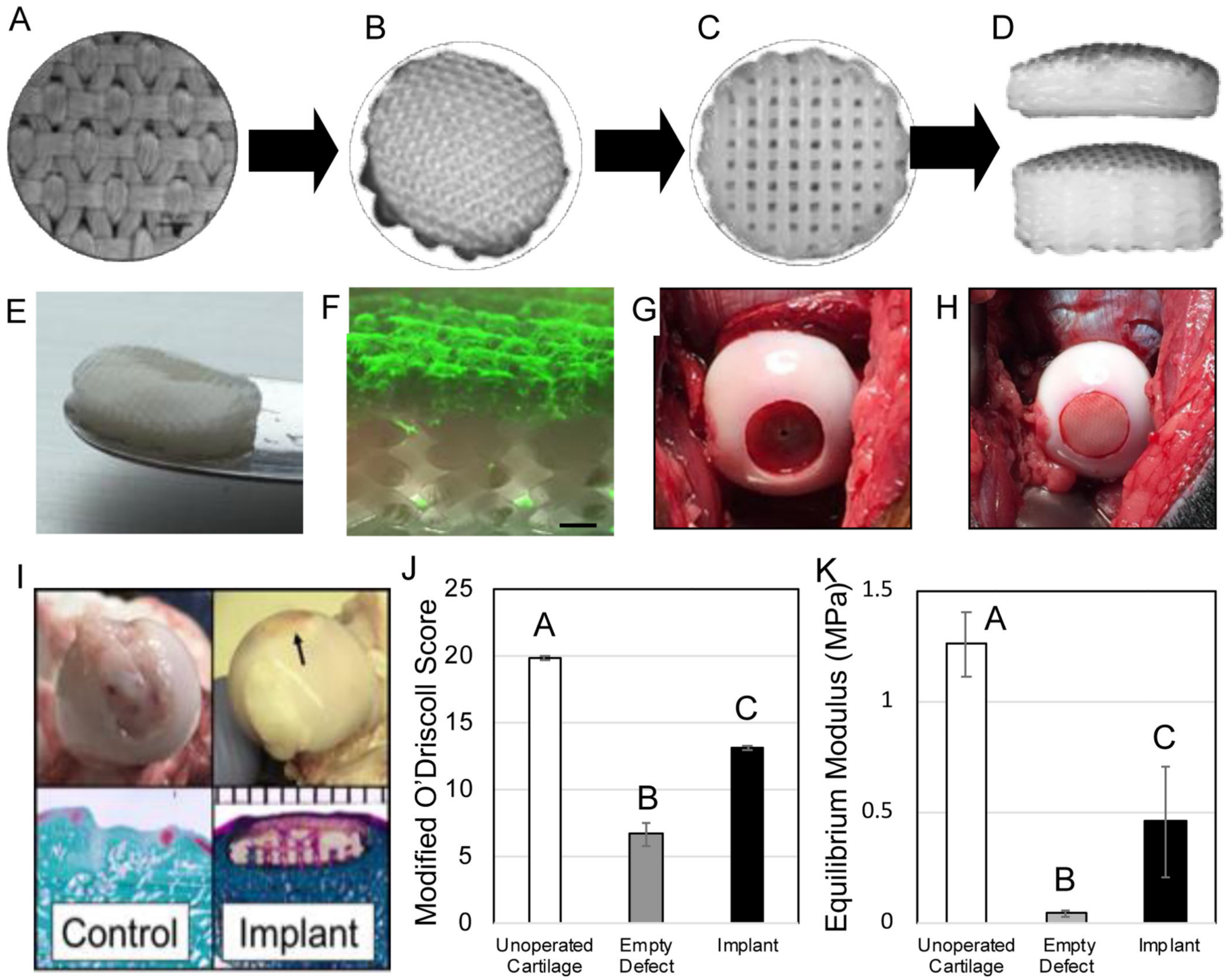

Figure 8.

Biological resurfacing in a large animal, preclinical model of hip osteoarthritis. (Top Row) Schematic of implant design. (A-B) Textile component is fused to the (C) additive manufactured component to form the (D) biocomponent implant of variable heights. (Middle row) Disposition of the implant at the time of implantation. (E) Gross image of implant (10mm diameter) that was seeded with autologously harvested canine MSCs and cultured in vitro for 18 days in chondrogenic conditions. Note smooth, cartilaginous tissue synthesized in upper surface layer. (F) Confocal image demonstrating viable ECM synthesis (fluorescent labeling for collagen) is confined to upper layer of bilayered implant (scale bar = 0.5 mm). (G) Intraoperative photograph of massive defect created in the femoral head, and (H) image immediately after placing the implant. (Bottom row) (I) Representative examples at necropsy of operated femoral heads at 6 months (arrow indicates location of implant). Safranin O and Fast Green (left) and Trichrome stain (right). Note that unstained section of each image is structural polymer. (J) Modified O'Driscoll scores and (K) elastic compressive equilibrium (Young's) modulus demonstrate a significant tissue repair (Groups not sharing the same letter are statistically different $*p<0.05$). Figure adapted from [91].